coatings

MDPI

Article

Effect of Macroscopic Composition on the Performance of Self-Compacting Concrete

He Liu [1,*], Wenxi Li [1], Haonan Zou [1], Wei Bian [2], Jingyi Zhang [3], Ji Zhang [4] and Peng Zhang [4]

[1] School of Transportation and Geomatics Engineering, Shenyang Jianzhu University, Shenyang 110168, China; 18512453100@163.com (W.L.); 15114147960@163.com (H.Z.)
[2] Key Laboratory of Highway Construction & Maintenance Technology in Loess Region, Shanxi Transportation Research Institute, Taiyuan 030006, China
[3] School of Civil Engineering, Shenyang Urban Construction University, Shenyang 110167, China; dq_zjy@syucu.edu.cn
[4] Liaoning New Development Highway Technology Maintenance Co., Ltd., Shenyang 110058, China; 13324131953@163.com (J.Z.); 19232408304@163.com (P.Z.)
* Correspondence: heliu@sizu.edu.cn

Abstract: In recent years, there has been significant interest in the development of self-compacting concrete (SCC). This study views SCC as a two-phase composite material and introduces a new aggregate spacing coefficient model based on the concept of Fullman's mean free path and stereological theory. The validity of the aggregate spacing coefficient model was verified. The relationship between the fine and coarse aggregate coefficients and the properties of SCC are revealed. The results show that the slump and slump flow of SCC increase as the fine and coarse aggregate coefficients increase. The coarse aggregate spacing coefficient has a significant influence on the compressive strength and drying shrinkage of SCC. A significant linear relationship between the coarse aggregate spacing coefficient and SCC dry shrinkage properties is revealed. Compared to the conditional mixing proportion method, which considers the aggregate volume as a control factor, the aggregate spacing coefficient takes into account the aggregate volume and gradation, which can more accurately reflect the characteristics of the aggregate. Meanwhile, this new perspective on the macroscopic composition of SCC provides insights into the controlling factors of its performance.

Keywords: self-compacting concrete; Fullman's mean free path; stereological theory; aggregate volume fraction; aggregate spacing coefficient

Academic Editor: Valeria Vignali

Received: 30 December 2024
Revised: 27 January 2025
Accepted: 28 January 2025
Published: 2 February 2025

Citation: Liu, H.; Li, W.; Zou, H.; Bian, W.; Zhang, J.; Zhang, J.; Zhang, P. Effect of Macroscopic Composition on the Performance of Self-Compacting Concrete. *Coatings* **2025**, *15*, 161. https://doi.org/10.3390/coatings15020161

1. Introduction

The concept of self-compacting concrete (SCC) was proposed at the end of the 20th century [1]. SCC is a kind of concrete that can be compacted under its own gravity. Even if there are dense steel bars, SCC can completely fill the formwork evenly without additional vibration [2]. As a kind of high-performance concrete, SCC has been developed for more than thirty years and has been widely studied by scholars. Many research results have been achieved in the areas of preparation technology [3], mix design methods [4], performance test evaluation [5], and engineering applications [6] of SCC. As the key properties of SCC, such as slump flow, compressive strength and dry shrinkage [7], all affect the quality of SCC, it is crucial to study the key influencing factors of SCC performance.

To investigate the correlation between the material composition and mix design of SCC and its properties, scholars have conducted numerous experiments and numerical simulations. Liu and Chen [8] emphasized that SCC performance was significantly related

to aggregate characteristics. Khaleel et al. [9,10] carried out test methods such as slump flow and L-box. The test results confirmed that as the maximum particle size of the coarse aggregate increases, the slump flow and passing ability of the SCC mixture descend and the compressive strength decreases. Krasna et al. [11] proposed factors influencing the compressive strength of SCC, including the particle size and coarse aggregate proportion. The results showed that with coarse aggregate proportion increases, the compressive strength of concrete increases. However, Liu [8,12] found that within a certain range, the maximum increase in particle size was beneficial to the compressive strength of SCC. Chen [13] established the relationship between slump flow and aggregate properties, which included the average particle size and volume of the aggregate. These results helped to develop the SCC design.

Zhao [14] defined a coarse aggregate gradation (A/B ratio, size 5–10 mm, coarse aggregate weight/size 10–20 mm for 4/6, 5/5, 6/4, 7/3). The results showed that with the change in the A/B ratio from 4/6 to 7/3, the initial slump flow, blocking, and segregation ratio of SCC decreased. Zhang [15] developed a model to predict the plastic viscosity threshold of the mixture. The model was forecasted according to the paste yield stress threshold, which was calculated by the coarse aggregate content of SCC. Results showed that a higher coarse aggregate content would lead to a lower yield stress and larger plastic viscosity. Santos [16] investigated the properties of SCC with different skeleton distribution forms. Compared with the discontinuous gradation skeleton SCC, the continuous gradation skeleton SCC showed better flowability and passing ability and higher early strength. However, both types of gradation demonstrated similar compressive strength at 365 days. Furthermore, the shape of the aggregate also affected SCC performance. As the content of the multi-angular elongated and flaky aggregate increases, the slump flow of the SCC mixture decreases [17]. Previous research focused on fresh and hardened properties of SCC using a traditional mix design and aggregate macroscopic morphology, which was tedious and time-consuming [18]. In addition, contradictions between the properties of high-performance concrete made SCC preparation more complicated.

Scholars have proposed another research idea regarding SCC as a two-phase composite material, such as aggregate and mortar. Su [19] presented a new method for SCC mix design. After determining the required aggregate, mortar was then filled into the aggregate voids. Basheerudeen [20] claimed that by maximizing the aggregate particles' packing density and cementitious materials, the concrete mixture performance was enhanced.

Researchers also simulated fluid–solid flow to study SCC, using the smoothed particle hydrodynamics (SPH) method [21]. Dhaheer [22] verified the ability of the SPH simulation method to predict the passing ability of SCC through steel bars gap. Alyhya [23] simulated the flow of SCC through a V-funnel by the three dimensional meshless smoothed particle hydrodynamics (SPH) method. The simulation results were consistent with the experimental results. Tran-Duc [24] revealed the relationship between concrete performance and coarse aggregate content by a simulation method. The results revealed that the yield stress and plastic viscosity of SCC were increased as the coarse aggregate content increased.

To summarize the above, the qualitative influence of aggregate properties on the performance of SCC has achieved many research results, such as the particle size, proportion, and gradation of aggregate. These research results have played a vital role in promoting the development of SCC. However, in the process of studying the performance of SCC, the traditional method mainly takes the aggregate volume as a parameter. Therefore, this paper establishes a model based on Fullman's mean free path and the theory of stereology. The concept of coarse and fine aggregate spacing coefficients is proposed, considering the aggregate volume and aggregate gradation at the same time. The validity of the coarse and fine aggregate spacing coefficients is verified. The quantitative relationship between the

aggregate spacing coefficient and various properties of SCC is revealed. These findings will help us to understand the relationship between SCC performance and macroscopic composition parameters, measuring the key performance of SCC in a more refined way.

2. Material and Methods

SCC was prepared using raw materials including P.O42.5 cement, S95 slag, polycarboxylate superplasticizer, methyl cellulose ether, water, fine aggregates (graded river sand), and coarse aggregates (limestone aggregate) with an average size of 4.75 mm to 20 mm. The apparent density of river sand was 2.65 g/cm^3, while the coarse aggregate was 2.73 g/cm^3. The particle gradation results for river sand and gravel are shown in Table 1.

Table 1. Screening results of river sand and gravel particle composition.

	Passing Screening Rate/%								
	0.15 mm	**0.3 mm**	**0.6 mm**	**1.18 mm**	**2.36 mm**	**4.75 mm**	**9.5 mm**	**16 mm**	**19 mm**
river sand	1.2	12.4	31.5	20.5	15.0	19.4	0	0	0
gravel	0	0	0	0	0.6	3.6	41.3	/	54.5
	Rate of particles passing through each sieve/%								
	0.15 mm	0.3 mm	0.6 mm	1.18 mm	2.36 mm	4.75 mm	9.5 mm	16 mm	19 mm
river sand	1.2	13.6	45.1	65.6	80.6	100	0	0	0
gravel	0	0	0	0	0.6	4.2	45.5	/	100

2.1. Mix Proportion

In order to investigate the impact of the spacing coefficients of coarse and fine aggregates on the workability of fresh concrete, as well as the compressive strength and shrinkage of SCC, a series of experiments were conducted. Concretes with different aggregate volume fractions and spacing coefficients were designed. The mix proportions of each group of specimens are shown in Table 2.

Table 2. Materials and mix proportion of each specimen.

Item.	**Cementitious Materials (kg/m^3)**			**Water (kg/m^3)**	**SP (kg/m^3)**	**Aggregate**			
	C	**FA**	**GGBS**			**Δ_{ca}**	**Δ_{fa}**	**m_{ca} (kg/m^3)**	**m_{fa} (kg/m^3)**
1	338	78	104	156	6.24	0.9–1.8	1.09–1.41	1156–733	564–458
2	338	78	104	156	6.24	1.0–1.6	0.93–1.47	1086–798	638–443
4	338	78	104	156	6.24	1.0–1.6	0.83–1.66	1086–798	694–400
5	338	78	104	156	6.24	0.9–1.75	1.27	1156–748	499

2.2. Test Method

The test methods in this study were generally categorized into two types: the workability of fresh concrete, characterized by slump and slump flow, and the hardened properties of SCC, characterized by the compressive strength and drying shrinkage performance of SCC.

2.2.1. Workability Test

According to Q/CR 596-2017 [25], the workability of concrete is measured by the slump and the slump flow test. After the collapse cylinder is lifted, the distance of the

SCC mixture falling down is the slump. The slump flow is the average of the maximum diameter of the slump flow surface and the diameter in the vertical direction from the beginning of the slump to when the SCC mixture stops flowing, as shown in Figure 1.

Figure 1. Test and calculation method of slump flow.

The slump flow is calculated according to Equation (1).

$$SF = \frac{d_1 + d_2}{2} \tag{1}$$

2.2.2. Compressive Strength Test

According to GB/T50081-2019 [26], the compressive strength of specimens with a size of 150 × 150 × 150 mm^3 were tested by a hydraulic universal testing machine; the loading rate was 0.5 MPa/s. The compressive strength is calculated according to Equation (2).

$$f_c = F/A \tag{2}$$

where f_c is compressive strength, MPa; F is the failure load, N; and A is the bearing area, mm^2.

2.2.3. Drying Shrinkage Test

The drying shrinkage test of SCC was performed according to GB/T50082-2009 [27]. Prism specimens sized 100 × 100 × 515 mm^3 were used, and two stainless steel sheets were pasted at both ends of each specimen. The shrinkage rate of concrete is calculated according to Formula (3).

$$\varepsilon_{st} = \frac{L_0 - L_t}{L_b} \tag{3}$$

where ε_{st} is the shrinkage rate; L_0 is the specimen initial length, mm; L_t is the specimen length at t area, mm; and L_b is the measuring scale distance, mm.

3. Establishment and Verification of Aggregate Spacing Model

3.1. Establishment of Aggregate Spacing Model

Concrete is a multi-component composite material consisting of coarse and fine aggregates, cement, water, and admixtures. This study considers SCC as a two-phase composite material consisting of coarse aggregate and mortar, with the coarse aggregate particles being uniformly dispersed in the continuous phase of mortar, as represented by Figure 2. Furthermore, considering the mortar as a two-phase material consisting of fine aggregate and cement paste, the macroscopic structure of concrete and mortar can be described by aggregate spacing. As an important characteristic parameter, aggregate spacing can be

characterized by the aggregate spacing coefficient, which has a significant influence on the workability, strength, and durability of SCC.

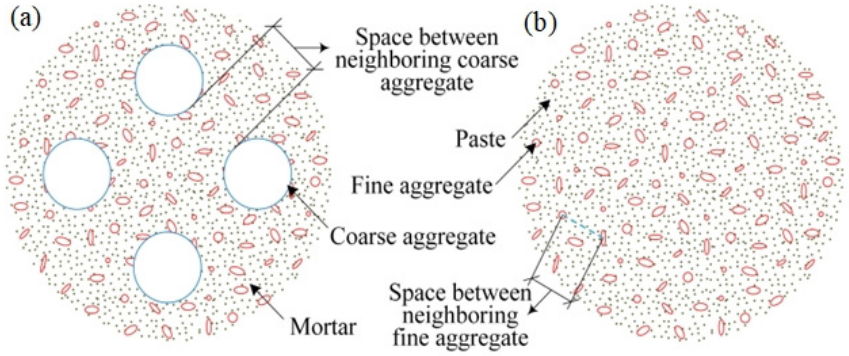

Figure 2. Schematics diagram of physical model for the compositions of cementitious material system. (**a**) concrete level, (**b**) mortar level.

When solving the distribution of solid particles and the distance between particles in a certain space system, the concept of Fullman's mean free path and the stereology theory are adopted. Therefore, we discussed the aggregate spacing coefficient based on the above theory [28,29]. For a binary composite system consisting of a dispersed phase of particles and a continuous phase, the mean free path between particles in the system can be calculated using the above theory. The calculation formula for the mean free path between particles in the system is shown in Equation (4).

$$\lambda = 4[1 - (V_V)_a]/(S_V)_a \tag{4}$$

where $(V_V)_a$ is the volume fraction of solid particle a in the unit volume binary system; $(S_V)_a$ is the surface area of solid particle a in the unit volume binary system, 1/m; and λ is the average free path between particles.

For the concrete system composed of mortar and coarse aggregate, if assuming that the maximum and minimum particle sizes of coarse aggregate are $D_{ca,max}$ and $D_{ca,min}$, respectively, the distribution of particle composition conforms to the Fuller distribution function, which is shown in Formula (5).

$$P_V(x) = (\sqrt{x} - \sqrt{D_{ca,\min}})/(\sqrt{D_{ca,\max}} - \sqrt{D_{ca,\min}}) \tag{5}$$

where $P_V(x)$ is the cumulative volume (or mass) fraction of coarse aggregate particles and x is the coarse aggregate diameter of the corresponding grain size.

Assuming that the total volume of the coarse aggregate particles is denoted as V_{ca}, the total surface area S_{ca} of the aggregate particles in this system can be expressed using Formula (6).

$$S_{ca} = \frac{6V_{ca}}{\sqrt{D_{ca,\max} \times D_{ca,\min}}} \tag{6}$$

By combining Formulas (4) and (6), we can derive the average spacing expression between adjacent coarse aggregate particle surfaces, which occurs in the binary system of concrete composed of mortar and coarse aggregate, as shown in Formula (7).

$$\lambda_{ca} = \frac{2(1 - V_{ca})}{3V_{ca}} \times \sqrt{D_{ca,\max} \times D_{ca,\min}} \tag{7}$$

If using Formula (8) to express the average particle diameter $d_{ca,av}$ of the particles in the coarse aggregate system and defining the average coarse aggregate spacing coefficient

Δ_{ca} as the ratio of the average spacing of adjacent coarse aggregates to the average diameter of the particles, then we can obtain the calculation formula of the coarse aggregate spacing coefficient in the concrete system, as shown in Formula (9):

$$d_{ca,av} = \frac{\sum_{i}^{n} d_{ca,i} m_{ca,i}}{\sum_{i}^{n} m_{ca,i}} \tag{8}$$

$$\Delta_{ca} = \frac{2(1 - V_{ca})}{3V_{ca}} \times \frac{\sqrt{D_{ca,\max} \times D_{ca,\min}}}{d_{ca,av}} \tag{9}$$

Similarly, we can obtain the spacing coefficient Δ_{fa} between sands in the mortar binary system, which is composed of sand fine aggregate and slurry, as shown in Formula (10).

$$\Delta_{fa} = \frac{2(1 - V_{fa})}{3V_{fa}} \times \frac{\sqrt{D_{fa,\max} \times D_{fa,\min}}}{d_{fa,av}} \tag{10}$$

where $d_{ca,I}$ and $m_{ca,i}$ represent the particle size and percentage of coarse aggregate for grade I, while $D_{ca,max}$, $D_{ca,min}$, and $D_{ca,av}$, represent the maximum, minimum, and average particle sizes of the coarse aggregate; $D_{fa,max}$, $D_{fa,min}$, and $D_{fa,av}$, represent the maximum, minimum, and average particle sizes of the fine aggregate; and V_{ca} and V_{fa} denote the volume fractions of coarse and fine aggregates, respectively.

Formulas (9) and (10) demonstrate that the coarse aggregate spacing coefficient in the concrete system is influenced by some factors, such as the volume fraction content and particle size distribution (maximum and minimum particle size, average particle size) of the coarse aggregate. Similarly, the fine aggregate spacing coefficient is influenced by the volume fraction content and particle size distribution of sand. Therefore, when the properties of cement paste and aggregate are certain, the aggregate spacing coefficient is closely related to the performance of concrete or mortar.

3.2. Validation of Aggregate Spacing Model

To verify the validity of the spacing coefficient aggregates, we tested the spacing coefficient of adjacent coarse aggregates. Firstly, we cut the SCC cube specimens with sizes of $100 \times 100 \times 100$ mm^3 into two equal parts by a cutting machine and polished the cutting surface until smooth. After the surface dried, each side was divided into three equal parts using a colored pen, and these parts were connected by four straight lines, as shown in Figure 3. Then, we measured the length of each coarse aggregate passing through each straight line using a steel ruler, with a minimum scale of millimeters, and calculated the total number of coarse aggregates passing through each straight line. The total length of coarse aggregate passing through each straight line was crossed with the total number of coarse aggregates, and then we divided the total length of the spacing on each straight line by the total number of coarse aggregates passing through it and added 1; this way, the average spacing coefficient Δ_{ca} of adjacent aggregates on each straight line can be obtained. Through the average spacing Δ_{ca} and the average diameter $d_{ca,av}$ of the coarse aggregate, the spacing coefficient of the adjacent coarse aggregate on each straight line can be calculated. The aggregate spacing was the aggregate spacing coefficient multiplied by the average particle size of the coarse aggregate. Finally, the test results for the arithmetic mean of aggregate spacing calculated on the four straight lines are obtained. The average spacing test diagram of the adjacent aggregates is shown in Figure 3.

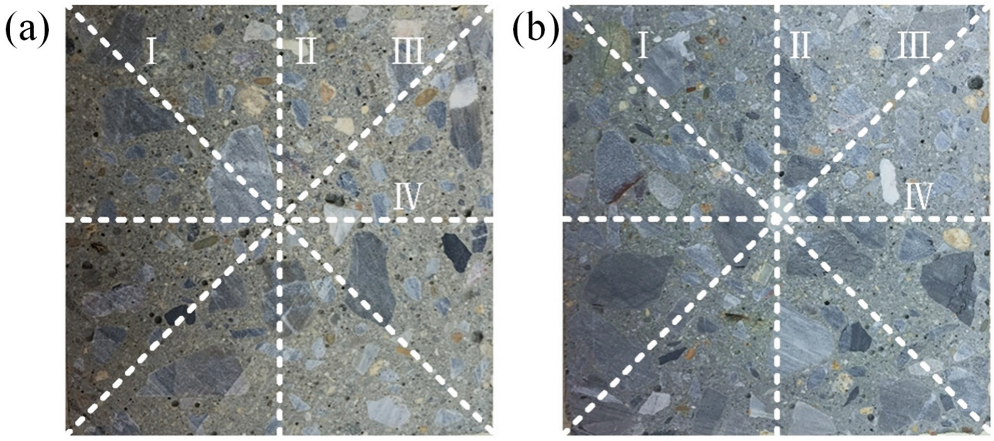

Figure 3. The average spacing test diagram of adjacent aggregates. (**a**) aggregate spacing coefficient 2.4, (**b**) aggregate spacing coefficient 1.8.

In Figure 3a, I is 8, II is 5, III is 8, IV is 6, $\lambda = (17.6 + 20 + 17.6 + 16.7)/4 = 18.6$ mm, the calculated value is $\Delta ca = 18.6/7.44 = 2.5$, and the error is 4.17%.

In Figure 3b, I is 10, II is 7, III is 10, IV is 8, $\lambda = (14.1 + 14.3 + 14.1 + 12.5)/4 = 13.8$ mm, the calculated value is $\Delta_{ca} = 13.8/7.44 = 1.85$, and the error is 2.78%.

The comparison between the test value and calculated value of the two specimens is shown in Figure 4.

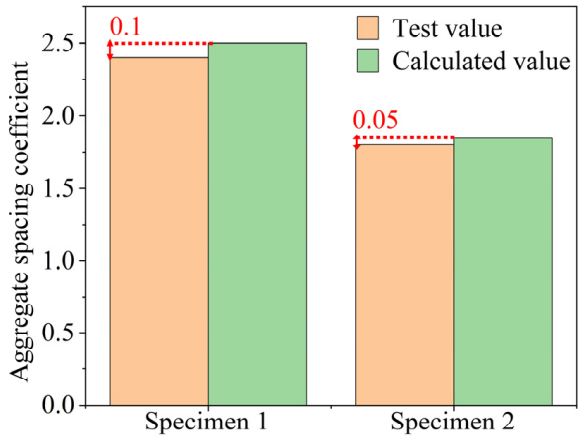

Figure 4. The comparison results of the calculated value and the test value of the aggregate spacing coefficient.

We calculated specimens with coarse or fine aggregate volume fractions of 0.1, 0.15, 0.2, 0.25, 0.3, 0.35, 0.4, 0.45, and 0.5. According to above method, the corresponding coarse or fine aggregate spacing coefficients were calculated. The relationship between the volume fraction and spacing coefficients is shown in Figure 5.

Figure 5 shows that for both coarse and fine aggregates, the corresponding spacing coefficient decreases as the aggregate volume fraction increases. In SCC, which is a two-phase composite system, more aggregate will lead to a smaller gap between aggregates.

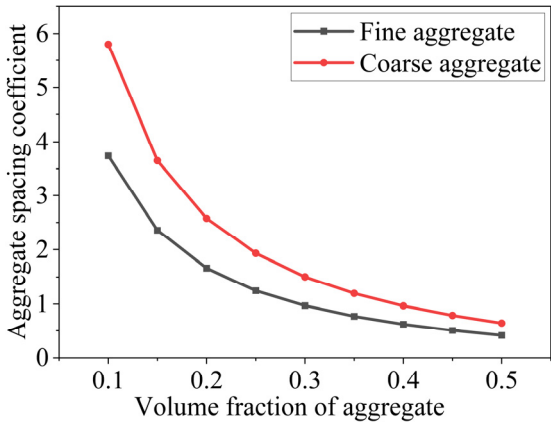

Figure 5. Relationship between the volume fraction of aggregate and the aggregate spacing coefficient in the system.

4. Result and Discussion

4.1. Workability of Fresh Concrete

SCC with fine aggregate spacing coefficients of 1.41, 1.27, and 1.09 when changing the coarse spacing coefficient from 0.9 to 1.8 was analyzed. The slump and slump flow of SCC were measured, as shown in Figure 6.

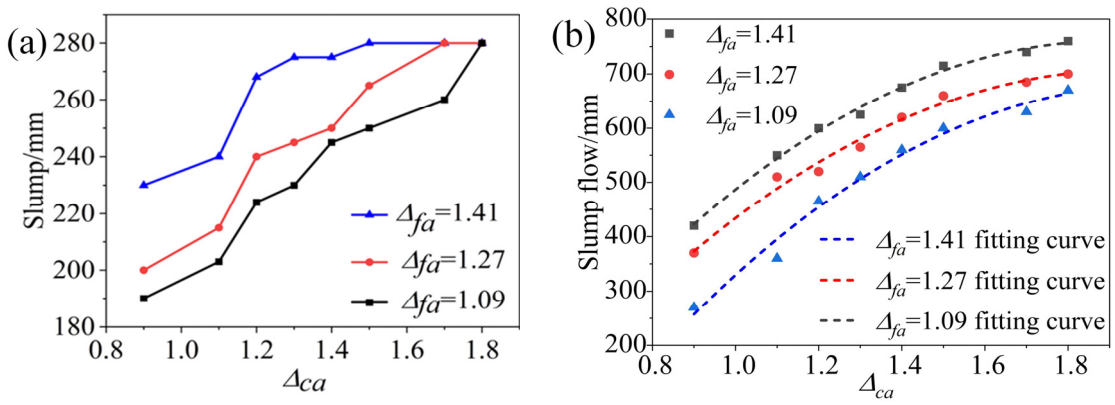

Figure 6. Relationship between coarse aggregate spacing coefficient and fluidity of fresh concrete. (**a**) Correlation between coarse aggregate spacing coefficient and slump, (**b**) correlation between coarse aggregate spacing coefficient and slump flow.

The results in Figure 6 demonstrate that when the fine aggregate spacing coefficient is 1.41, 1.27, and 1.09, the slump and slump flow of fresh SCC increase as the coarse aggregate spacing coefficient increases. The coarse aggregate particles disperse uniformly in the mortar continuous phase with a certain spacing. The larger the coarse aggregate spacing, the more mortar can flow over the coarse aggregate in the system and the better the flowability performance.

Figure 6a illustrates that for the mixture with an aggregate spacing coefficient of 1.41, when the coarse aggregate spacing coefficient increased to 1.3, the slump no longer increased and remained at 280 mm. Similarly, the slump of the mixture with a fine aggregate spacing coefficient of 1.27 also increased to 280 mm and remained unchanged. At this time, the coarse aggregate spacing coefficient was 1.5. This shows that when the slump increases to 280 mm, the workability of the SCC mixture cannot be accurately reflected. Figure 6b illustrates that the three types of fresh SCC all have the same trend; that is, they increase continuously with the coarse spacing coefficient. For the mixture with the fine aggregate spacing coefficient of 1.09, the slump flow increases most rapidly with the coarse

aggregate spacing coefficient being between 1.1 and 1.2, and the growth rate is slow with the coarse aggregate spacing coefficient being between 0.8 and 1.1. For the mixture with the fine aggregate spacing coefficient of 1.27, the slump flow increases most rapidly with the coarse aggregate spacing coefficient being between 0.8 and 1.1, and the growth rate is slow between 1.1 and 1.2. The growth rate of the mixture slump flow is essentially unchanged, with a fine aggregate spacing coefficient of 1.09 when the coarse aggregate spacing coefficient is between 0.8 and 1.2. This is mainly because the fiction between aggregates decreases when the coarse aggregate spacing coefficient increases. This leads to the concrete dissipating less energy. This also increases the slump of SCC.

When the fine aggregate spacing coefficients are 1.41, 1.27, and 1.09, respectively, the fitting relationship between the coarse aggregate spacing coefficient and the fluidity of fresh SCC is shown in Table 3.

Table 3. Relationship between coarse aggregate spacing and SCC fluidity.

Δ_{fa}	Fitting Formula
1.41	$SF = -337.65\Delta_{ca}^2 + 1282.98\Delta_{ca} - 458.66$
1.27	$SF = -304.06\Delta_{ca}^2 + 1184.93\Delta_{ca} - 446.97$
1.09	$SF = -339.83\Delta_{ca}^2 + 1369.96\Delta_{ca} - 700.45$

Fresh SCC with fine aggregate spacing coefficients of 1.0, 1.3, and 1.6 was analyzed. The slump and slump flow of SCC were measured, as shown in Figure 7.

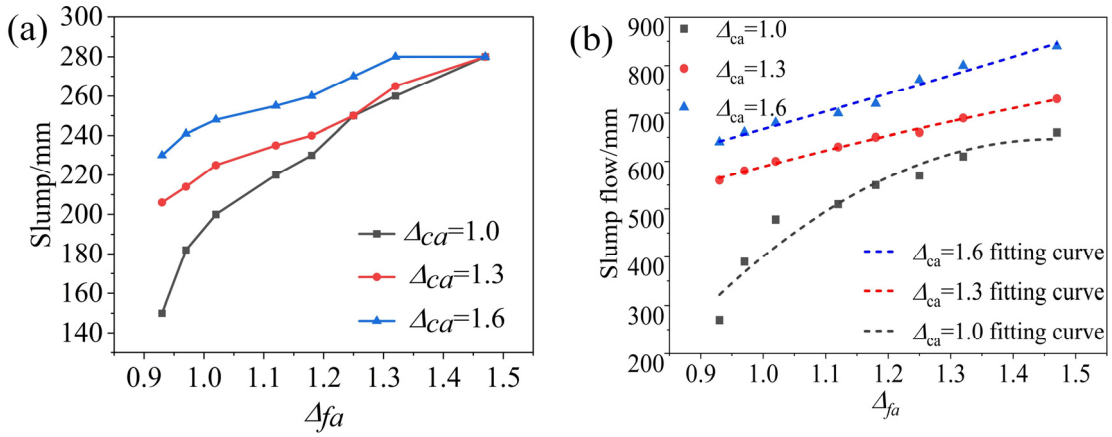

Figure 7. Relationship between fine aggregate spacing coefficient and fluidity of fresh concrete. (**a**) Correlation between fine aggregate spacing coefficient and slump, (**b**) correlation between fine aggregate spacing coefficient and slump.

The results in Figure 7 illustrate that the coarse aggregate spacing remains at 1.0, 1.3, and 1.6. The slump and slump flow of fresh SCC increase as the fine aggregate spacing coefficient increases. In the mortar system, fine aggregates are uniformly suspended in the cement paste. A higher spacing coefficient of the fine aggregates leads to a smaller fine aggregate volume fraction, an increase in the cement paste content, and a higher flowability of fresh SCC.

As shown in Figure 7a, the slump of SCC with a coarse aggregate spacing coefficient of 1.6 is most affected by the fine aggregate spacing coefficient. In addition, SCC with a coarse aggregate spacing coefficient of 1.0 is stable; when the slump increases to 280 mm, it no longer increases with the increase in the fine aggregate spacing coefficient. The slump flow of SCC increases as the fine aggregate spacing coefficient increases, as shown in Figure 7b. The SCC with a coarse aggregate spacing coefficient of 1.3 grows the most uniformly. When the fine aggregate spacing is between 1.02 and 1.18, SCC with a coarse

aggregate spacing coefficient of 1.0 slowly increases, and then it grows rapidly. When the fine aggregate spacing is between 0.93 and 1.02, the slump flow of SCC with an aggregate spacing coefficient of 1.6 increases rapidly and then slows down.

The coarse aggregate spacing coefficients are 1.6, 1.3, and 1.0. The fitting relationship between the fine aggregate spacing coefficient and the slump of fresh SCC is shown in Table 4.

Table 4. Relationship between fine aggregate spacing and SCC slump.

Δ_{fa}	Fitting Formula
1.6	$SF = -32.16\Delta_{fa}^2 + 301.48\Delta_{fa} - 333.23$
1.3	$SF = -93.50\Delta_{fa}^2 + 528.56\Delta_{fa} - 153.77$
1.0	$SF = -1132.61\Delta_{fa}^2 + 3319.33\Delta_{fa} - 1785.86$

The flow process of SCC could be regarded as the conversion of gravitational potential energy to friction energy and kinetic energy. With the increase in the coarse aggregate spacing coefficient, the friction between aggregates decreases; that is, the energy dissipated by the concrete phase decreases and more gravitational potential energy is converted into kinetic energy, which makes the mixture flow better. However, in the process of increasing the fine aggregate spacing, the fine aggregate volume and surface area decrease and the water adsorbed on the surface of aggregate decreases, which leads to a decrease in SCC viscosity and better flow.

4.2. Compressive Strength of Concrete

Figure 8 shows the compressive strength of SCC specimens with different coarse aggregate spacing coefficients and different fine aggregate spacing coefficients.

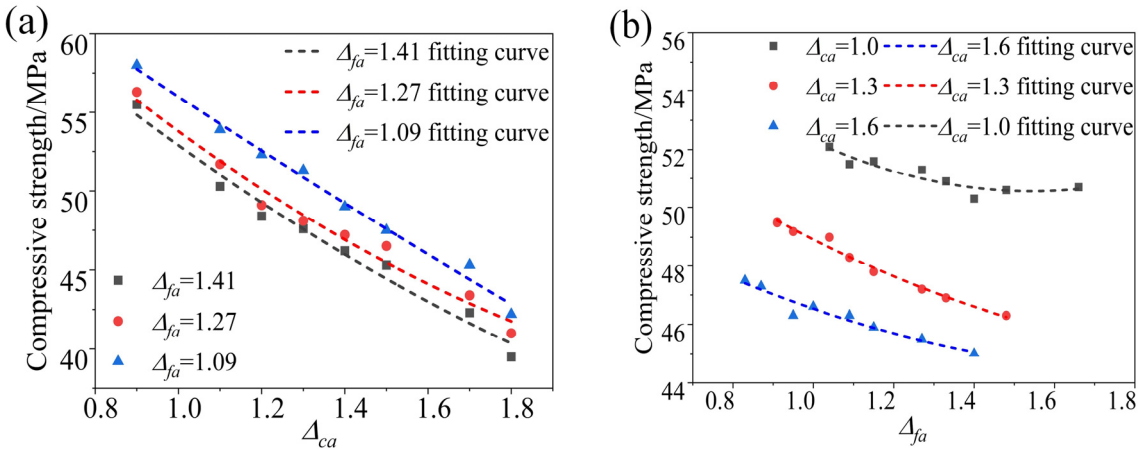

Figure 8. Relationship between aggregate spacing coefficients and compressive strength of SCC. (**a**) Correlation between coarse aggregate spacing coefficient and compressive strength, (**b**) correlation between fine aggregate spacing coefficient and compressive strength.

Figure 8a shows that when the fine aggregate spacing coefficients are 1.09, 1.27, and 1.41, the compressive strength of SCC specimens decreases with the increase in the coarse aggregate spacing coefficients, which decrease by 28.83%, 27.18%, and 27.24%, respectively. The fitting relationship between coarse aggregate spacing coefficients and the compressive strength of SCC is shown in Table 5.

Table 5. Relationship between coarse aggregate spacing and SCC compressive strength.

Δ_{fa}	Fitting Formula
1.41	$\sigma = 4.09\Delta_{ca}^2 - 27.11\Delta_{ca} + 75.92$
1.27	$\sigma = 5.44\Delta_{ca}^2 - 30.27\Delta_{ca} + 78.62$
1.09	$\sigma = 1.25\Delta_{ca}^2 - 19.96\Delta_{ca} + 74.70$

When the coarse aggregate spacing coefficients are 1.0, 1.3, and 1.6, the fitting relationship between the fine aggregate spacing coefficient and the compressive strength of SCC is as shown in Table 6. As shown in Figure 8b, the compressive strength of SCC with coarse aggregate spacing coefficients of 1.0, 1.3, and 1.6 decreases by 2.69%, 6.46%, and 5.26%, respectively.

Table 6. Relationship between fine aggregate spacing and SCC compressive strength.

Δ_{ca}	Fitting Formula
1.6	$\sigma = 2.52\Delta_{fa}^2 - 9.73\Delta_{fa} + 53.74$
1.3	$\sigma = 2.98\Delta_{fa}^2 - 12.97\Delta_{fa} + 58.91$
1.0	$\sigma = 5.86\Delta_{fa}^2 - 18.10\Delta_{fa} + 64.52$

Comparing Figure 8a,b, the variation in the coarse aggregate spacing coefficient has a more significant effect on SCC compressive strength. This is because the strength of SCC is influenced by the skeleton, which is composed of coarse aggregate. The fine aggregate is mainly used to fill the skeleton gap. As the coarse aggregate spacing coefficient increases, the volume fraction decreases and the skeleton cannot be formed, resulting in a significant decrease in strength.

When the aggregate spacing is small, the locked skeleton structure can be formed between the aggregates, which can provide greater strength when the SCC is under pressure. When the aggregate spacing increases, the locking force decreases, resulting in a decrease in SCC strength.

4.3. Drying Shrinkage of SCC

The shrinkage at different ages for different aggregate spacing coefficients is as shown in Figure 9.

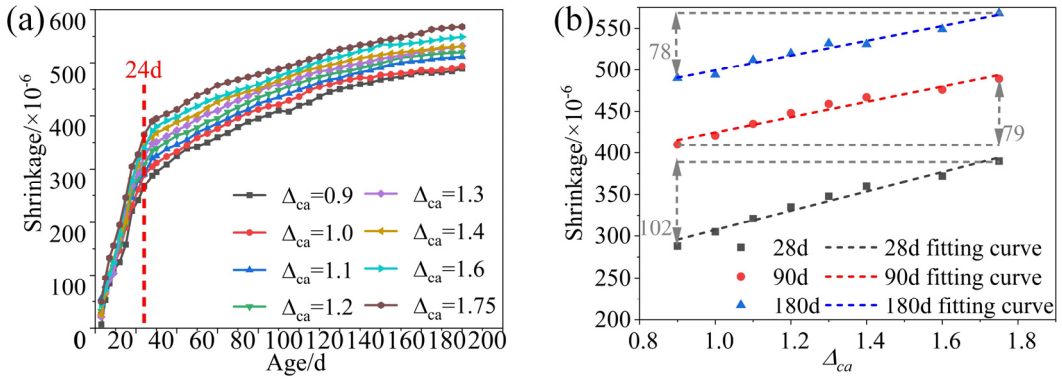

Figure 9. Relationship between aggregate spacing coefficient and drying shrinkage of concrete. (**a**) Correlation between curing age and drying shrinkage, (**b**) correlation between coarse aggregate spacing coefficient and drying shrinkage.

Figure 9a illustrates the drying shrinkage development of SCC with varying coarse aggregate spacing coefficients, from 0.9 to 1.75. As the coarse aggregate spacing coefficient increases, the shrinkage of SCC will increase gradually.

In SCC, the aggregates are inert materials and the main shrinkage is generated by the paste. As the aggregate spacing increases, the aggregate volume decreases, resulting in the inert phase volume decreasing, leading to an increase in the shrinkage of SCC.

Figure 9b illustrates the shrinkage of SCC under different coarse aggregate spacing coefficients, with ages of 28 days, 90 days, and 180 days. As the coarse aggregate spacing coefficient increases, the shrinkage of SCC at three different ages increases, where the shrinkage at 28 days is the largest. The shrinkage at 90 days increased by 79×10^{-6}, and the SCC shrinkage at 180 days increased the least, which was 78×10^{-6}.The changes in shrinkage values at 90 days and 180 days were very similar, which further shows that shrinkage develops rapidly in the early stage and slows down in the later stage.

The relationships between the coarse aggregate spacing coefficient and the drying shrinkage of SCC at different ages were fitted. The results are presented in Table 7.

Table 7. Relationship between coarse aggregate spacing and SCC drying shrinkage.

Age.	Fitting Formula
180 d	$y = 116.20\Delta_{ca} + 191.00$
90 d	$y = 91.79\Delta_{ca} + 333.02$
28 d	$y = 89.17\Delta_{ca} + 410.25$

In addition, according to Figure 9b, the drying shrinkage of SCC increases with the increase in the coarse aggregate spacing coefficient. As the coarse aggregate spacing coefficient increases, the volume fraction will decrease, leading to the need to fill the gap in the coarse aggregate. Therefore, the water content in the SCC suspension system increases, resulting in a large drying shrinkage of SCC.

5. Conclusions

In this paper, a model was established based on Fullman's mean free path and stereological theory, and the relationship between the aggregate volume and aggregate spacing coefficient was proposed. The quantitative relationship between aggregate spacing and various properties of SCC was obtained through experiments. The following conclusions can be drawn:

(1) A new aggregate spacing model was proposed. By comparing the results of the calculated value and the test value of the aggregate spacing coefficient, the validity of the model is verified.

(2) The slump and the slump flow of SCC increases as the aggregate spacing coefficient increases. The slump was maintained at 280 mm and then no longer decreased significantly, while the slump flow continued to increase.

(3) With the increase in the aggregate spacing coefficient, the compressive strength of SCC obviously decreased. And compared with the fine aggregate, the increase in the coarse aggregate spacing coefficient was more obvious in the decrease in compressive strength.

(4) An increase in the aggregate spacing coefficient will result in a significant increase in the drying shrinkage of SCC, which showed the fastest development in the early stage (3 d–24 d), slowing down in the later stage (24 d–180 d).

(5) In practical applications, for the case of different steel bar spacings in the project, choosing SCC with different aggregate spacing coefficients can make the design more convenient and accurate.

Author Contributions: Data curation, Funding acquisition, Methodology, Project administration, Supervision, Writing—original draft, H.L.; Investigation, Writing—original draft, Writing—review and

editing, W.L.; Investigation, Original draft preparation, Data curation, H.Z.; Project ad-ministration, Formal analysis, Review and editing, W.B.; Writing—original draft, Writing—review and Editing, J.Z. (Jingyi Zhang); Supervision and Validation, J.Z. (Ji Zhang); Original draft preparation, Data curation, P.Z. All authors have read and agreed to the published version of the manuscript.

Funding: This work was supported by Key Laboratory of Highway Construction and Maintenance Technology in Loess Region, Ministry of Transport, PRC (KLTLR-Y23-10); Foundation of Liaoning Province Education Administration (grant numbers JYTMS20231556) and Liaoning transportation technology project (grant number: 202328).

Institutional Review Board Statement: Not applicable.

Informed Consent Statement: Not applicable.

Data Availability Statement: The data presented in this study are available on request from the corresponding author.

Conflicts of Interest: Ji Zhang and Peng Zhang were employed by the Liaoning New Development Highway Technology Maintenance Co., Ltd. The remaining authors declare that the research was conducted in the absence of any commercial or financial relationships that could be construed as a potential conflict of interest.

References

1. Okamura, H.; Ouchi, M. Self-compacting high performance concrete. *Prog. Struct. Eng. Mater.* **1998**, *1*, 378–383. [CrossRef]
2. Okamura, H.; Ozawa, K. Self-Compacting High Performance Concrete. *Struct. Eng. Int.* **1996**, *6*, 269–270. [CrossRef]
3. Liu, S.H. Key Techniques of Self-Compacting Concrete. *Adv. Mater. Res.* **2011**, *261–263*, 394–397. [CrossRef]
4. Shi, C.; Wu, Z.; Lv, K.; Wu, L. A review on mixture design methods for self-compacting concrete. *Constr. Build. Mater.* **2015**, *84*, 387–398. [CrossRef]
5. Goodier, C.I. Development of self-compacting concrete. *Proc. Inst. Civ. Eng.—Struct. Build.* **2003**, *156*, 405–414. [CrossRef]
6. Henault, J.W. Self-Consolidating Concrete: A Synthesis of Research Findings and Best Practices. *Lit. Rev.* **2014**, *8*, 11–20. [CrossRef]
7. Cu, Y.T.H.; Tran, M.V.; Ho, C.H.; Nguyen, P.H. Relationship between workability and rheological parameters of self-compacting concrete used for vertical pump up to supertall buildings. *J. Build. Eng.* **2020**, *32*, 101786. [CrossRef]
8. Liu, H.Q.; Chen, X. Influence of Aggregate on Workability of Self-Compacting Concrete. *Adv. Mater. Res.* **2012**, *482–484*, 1101–1104. [CrossRef]
9. Khaleel, O.; Al-Mishhadani, S.; Razak, H.A. The Effect of Coarse Aggregate on Fresh and Hardened Properties of Self-Compacting Concrete (SCC). *Procedia Eng.* **2011**, *14*, 805–813. [CrossRef]
10. Shobha, M.; Mohan, D.H.; Raju, P.S.N. Aggregate size and behaviour of self-compacting concrete. *Proc. Inst. Civ. Eng.—Constr. Mater.* **2006**, *159*, 147–152. [CrossRef]
11. Dehestani, M.; Nikbin, I.; Asadollahi, S. Effects of specimen shape and size on the compressive strength of self-consolidating concrete (SCC). *Constr. Build. Mater.* **2014**, *66*, 685–691. [CrossRef]
12. Nikbin, I.; Beygi, M.; Kazemi, M.; Amiri, J.V.; Rahmani, E.; Rabbanifar, S.; Eslami, M. A comprehensive investigation into the effect of aging and coarse aggregate size and volume on mechanical properties of self-compacting concrete. *Mater. Des.* **2014**, *59*, 199–210. [CrossRef]
13. Ma, K.; Feng, J.; Long, G.; Xie, Y.; Chen, X. Improved mix design method of self-compacting concrete based on coarse aggregate average diameter and slump flow. *Constr. Build. Mater.* **2017**, *143*, 566–573. [CrossRef]
14. Zhao, H.; Sun, W.; Wu, X.; Gao, B. The effect of coarse aggregate gradation on the properties of self-compacting concrete. *Mater. Des.* **2012**, *40*, 109–116. [CrossRef]
15. Zhang, J.; An, X.; Yu, Y.; Nie, D. Effects of coarse aggregate content on the paste rheological thresholds of fresh self-compacting concrete. *Constr. Build. Mater.* **2019**, *208*, 564–576. [CrossRef]
16. Santos, A.C.; Ortiz-Lozano, J.A.; Villegas, N.; Aguado, A. Experimental study about the effects of granular skeleton distribution on the mechanical properties of self-compacting concrete (SCC). *Constr. Build. Mater.* **2015**, *78*, 40–49. [CrossRef]
17. Wu, J.; Jia, Z.; Zhou, X. Discrete element analysis of the effect of aggregate morphology on the flowability of self-compacting concrete. *Case Stud. Constr. Mater.* **2023**, *18*. [CrossRef]
18. Chen, B.; Wang, L.; Feng, Z.; Liu, Y.; Wu, X.; Qin, Y.; Xia, L. Optimization of high-performance concrete mix ratio design using machine learning. *Eng. Appl. Artif. Intell.* **2023**, *122*. [CrossRef]
19. Su, N.; Hsu, K.-C.; Chai, H.-W. A simple mix design method for self-compacting concrete. *Cem. Concr. Res.* **2001**, *31*, 1799–1807. [CrossRef]

20. Basheerudeen, A.; Anandan, S. Particle Packing Approach for Designing the Mortar Phase of Self Compacting Concrete. *Eng. J.* **2014**, *18*, 127–140. [CrossRef]
21. Feiguo, C.; Wei, G. A review of smoothed particle hydrodynamics family methods for multiphase flow. *Chin. J. Theor. Appl. Mech.* **2021**, *53*, 2357–2373. [CrossRef]
22. Dhaheer, M.A.; Kulasegaram, S.; Karihaloo, B. Simulation of self-compacting concrete flow in the J-ring test using smoothed particle hydrodynamics (SPH). *Cem. Concr. Res.* **2016**, *89*, 27–34. [CrossRef]
23. Alyhya, W.; Kulasegaram, S.; Karihaloo, B. Simulation of the flow of self-compacting concrete in the V-funnel by SPH. *Cem. Concr. Res.* **2017**, *100*, 47–59. [CrossRef]
24. Tran-Duc, T.; Ho, T.; Thamwattana, N. A smoothed particle hydrodynamics study on effect of coarse aggregate on self-compacting concrete flows. *Int. J. Mech. Sci.* **2020**, *190*, 106046. [CrossRef]
25. *Q/CR 596-2017*; Specification of Self-Compacting Concrete for High-Speed Railway CRTSIII Slab Ballastless Track. China Railway Press: Beijing, China, 2019.
26. *GB/T 50081-2019*; Standard for Test Methods of Concrete Physical and Mechanical Properties. Ministry of Housing and Urban-Rural Development of the People's Republic of China: Beijing, China, 2019.
27. *GB/T 50082-2009*; Standard for Test Methods of Long-Term Performance and Durability of Ordinary Concrete. China Construction Industry Press: Beijing, China, 2009.
28. Chen, H.S.; Sun, W.; Stroeven, P. Regular dodecahedron model to calculate the average surface spacing between the nearest neighboring aggregate grains concrete. *J. Chin. Ceram. Soc.* **2003**, *31*, 1048–1052. [CrossRef]
29. Chen, H.S.; Sun, W.; Stroeven, P.; Stroeven, M. Stereological method of calculatmg the average value of surface spacing be-tween the neighboring aggregate grains in concrete. *J. Harbin Inst. Technol.* **2005**, *37*, 1511–1514.